American Journal of Pathology, Vol. 163, No. 3, September 2003

Hypermethylation of the Human Glutathione *S*-Transferase-π Gene (*GSTP1*) CpG Island Is Present in a Subset of Proliferative Inflammatory Atrophy Lesions but Not in Normal or Hyperplastic Epithelium of the Prostate

A Detailed Study Using Laser-Capture Microdissection

Masashi Nakayama,* Christina J. Bennett,* Jessica L. Hicks,* Jonathan I. Epstein,*†‡ Elizabeth A. Platz,†‡§ William G. Nelson,*†‡ and Angelo M. De Marzo*†‡

From the Department of Pathology, the Brady Urological Institute,† the Sidney Kimmel Comprehensive Cancer Center at Johns Hopkins,‡ and the Bloomberg School of Public Health,§ the Johns Hopkins Medical Institutions, Baltimore, Maryland*

Somatic inactivation of the glutathione *S*-transferase-π gene (*GSTP1*) via CpG island hypermethylation occurs early during prostate carcinogenesis, present in ~70% of high-grade prostatic intraepithelial neoplasia (high-grade PIN) lesions and more than 90% of adenocarcinomas. Recently, there has been a resurgence of the concept that foci of prostatic atrophy (referred to as proliferative inflammatory atrophy or PIA) may be precursor lesions for the development of prostate cancer and/or high-grade PIN. Many of the cells within PIA lesions contain elevated levels of GSTP1, glutathione *S*-transferase-α (GSTA1), and cyclooxygenase-II proteins, suggesting a stress response. Because not all PIA cells are positive for GSTP1 protein, we hypothesized that some of the cells within these regions acquire *GSTP1* CpG island hypermethylation, increasing the chance of progression to high-grade PIN and/or adenocarcinoma. Separate regions (n =199) from 27 formalin-fixed paraffin-embedded prostates were microdissected by laser-capture microdissection (Arcturus PixCell II). These regions included normal epithelium (n = 48), hyperplastic epithelium from benign prostatic hyperplasia nodules (n = 22), PIA (n = 64), high-grade PIN (n = 32), and adenocarcinoma (n = 33). Genomic DNA was isolated and assessed for *GSTP1* CpG island hypermethylation by methylation-specific polymerase chain reaction. *GSTP1* CpG island hypermethylation was not detected in normal epithelium (0 of 48) or in hyperplastic epithelium (0 of 22), but was found in 4 of 64 (6.3%) PIA lesions. The difference in the frequency of *GSTP1* CpG island hypermethylation between normal or hyperplastic epithelium and PIA was statistically significant (P = 0.049). Similar to studies using nonmicrodissected cases, hypermethylation was found in 22 of 32 (68.8%) high-grade PIN lesions and in 30 of 33 (90.9%) adenocarcinoma lesions. Unlike normal or hyperplastic epithelium, *GSTP1* CpG island hypermethylation can be detected in some PIA lesions. These data support the hypothesis that atrophic epithelium in a subset of PIA lesions may lead to high-grade PIN and/or adenocarcinoma. Because these atrophic lesions are so prevalent and extensive, even though only a small subset contains this somatic DNA alteration, the clinical impact may be substantial. *(Am J Pathol 2003, 163:923–933)*

Various focal atrophic lesions involving prostatic epithelium have been described by a diverse range of terminology.[1] Recently Ruska and colleagues[2] simplified the classification of most of these lesions, referring to them as simple atrophy or postatrophic hyperplasia. McNeal[3] referred to similar focal lesions as postinflammatory atrophy, to emphasize the finding that most of these areas showed signs of ongoing or remote chronic inflammation. To highlight the fact that these atrophic foci in the pros-

Supported by the Public Health Service (grants NIH/NCI R01CA084997, NIH R01CA70196, and NIH/NCI Specialized Program in Research Excellence in Prostate Cancer P50CA58236 to The Johns Hopkins University).

Accepted for publication May 14, 2003.

Address reprint requests to Angelo M. De Marzo, M.D., Ph.D., Bunting-Blaustein Cancer Research Building, Room 153, 1650 Orleans St., Baltimore, MD 21231. E-mail: ademarz@jhmi.edu.

tate tend to be highly proliferative and are associated with inflammation, we termed these lesions "proliferative inflammatory atrophy" (PIA).[4] Long-term chronic inflammation may contribute to carcinogenesis in many organ systems through a postulated mechanism of repetitive tissue damage and regeneration in the presence of reactive phagocyte-derived oxygen and nitrogen species and cytokines.[5] That these lesions are incurring oxidative stress is suggested by the fact that expression of glutathione *S*-transferase π (GSTP1) and α (GSTA), enzymes typically induced in response to oxidative or electrophilic stresses, are elevated in PIA.[4,6] Also, cyclooxygenase II, another stress-inducible enzyme, is elevated in PIA.[7] Several investigators in the early part of the last century suggested that focal prostatic atrophy may be a precursor to prostate cancer by virtue of the predilection for both lesions to occur in the peripheral zone and their frequent occurrence near carcinoma lesions.[8,9] Franks[10] and Liavag[11] postulated that at least some forms of atrophy might directly give rise to cancer in the prostate. Recent morphological, immunohistochemical, and molecular-genetic evidence have provided preliminary support for this concept.[4,12–15] For example, atrophic epithelium in PIA is frequently found to merge directly with, and display morphological transitions to, high-grade PIN[12] and is often found near small carcinoma lesions.[10–12] In addition, some atrophic lesions have been shown to acquire somatic chromosome 8 abnormalities[13,15] and p53 mutations[14]—genetic changes that are associated with prostate cancer and high-grade PIN.

GSTP1, encoding glutathione *S*-transferase-π, has been proposed to be a caretaker gene, protecting cells against genome damage mediated by oxidants and electrophiles from inflammation or dietary exposures.[16–18] In the human prostate, the vast majority of high-grade PIN and prostatic adenocarcinoma lesions fail to express GSTP1, whose loss is associated with hypermethylation of the CpG island encompassing the *GSTP1* promoter. Methylation changes at this site have been detected in up to 100% of prostate cancer DNA specimens[16,19–32] and in ~70% of high-grade PIN,[24,28,30,32,33] but are generally not found in normal prostate tissue. Although many of the luminal epithelial cells in PIA lesions express GSTP1, some do not.[4] We hypothesize that some PIA cells may acquire *GSTP1* CpG island hypermethylation leaving these cells vulnerable to progress to high-grade PIN and/or adenocarcinoma. Because atrophic cells expressing GSTP1 would not be expected to harbor *GSTP1* promoter hypermethylation, and because the majority of the tissue within areas of PIA is stromal, we needed a method to enrich the epithelial cells in these regions to perform molecular analysis. For this, we isolated selected cell populations using laser-capture microdissection (LCM). Here, we report the results of a large survey of human clinical prostate tissues that examined the methylation status of the *GSTP1* CpG island in matched samples of normal prostate, epithelial benign prostatic hyperplasia (BPH) tissue, PIA, high-grade PIN, and prostatic adenocarcinoma.

Materials and Methods

Prostate Tissue Samples

Twenty-seven formalin-fixed paraffin-embedded radical prostatectomy specimens were randomly selected from a larger series of patients who underwent radical retropubic prostatectomy for clinically localized prostate adenocarcinoma at The Johns Hopkins Hospital between 2000 and 2001. All patients provided informed consent for use of tissues, and the use of tissues was approved by the Johns Hopkins University School of Medicine Institutional Review Board. The median patient age was 59-years-old and ranged from 47 to 67 years. The median preoperative serum prostate specific antigen (PSA) was 5.5 (range, 4.0 to 11.5). The median Gleason score was 6 (range, 5 to 8) and the pathological stage ranged from pT2N0Mx to pT3aN0Mx. A series of a 5-μm sections and two 10-μm sections were cut from each tissue block. A 5-μm section was hematoxylin and eosin (H&E)-stained for pathological evaluation to identify each region. One or two 10-μm sections were used for LCM. Adjacent sections in some cases were stained by immunohistochemistry for 34βE12 and/or GSTP1.

Histological Classification of Normal and Hyperplastic Tissues

Epithelium was classified as histologically normal when glands contained two epithelial cell layers lined by luminal cells that were tall and columnar. These luminal cells contained pale-to-clear cytoplasm and nuclei that were generally round, mostly basally located, and nearly even in size and shape and showed either no evidence of nucleoli or only very small nucleoli (<1 μm). These normal appearing glands contained abundant papillary infoldings and were generally lined by a continuous or mostly continuous basal cell layer. Epithelium was classified as hyperplastic when a similar histological appearance to that of normal epithelium, albeit at times with more pronounced papillae, was seen and the region occurred within an enlarged nodule in the transitional zone (nodular hyperplasia or benign prostatic hyperplasia).[3]

Histological Classification of PIA

We classified PIA lesions into the following types: simple atrophy, postatrophic hyperplasia, or mixed simple atrophy/postatrophic hyperplasia.[2] Simple atrophy consists of atrophic cells lining acini with relatively normal caliber that lack papillary fronds, where the number of glands per unit area do not appear to be increased relative to normal tissue. Postatrophic hyperplasia consists of acini that are smaller and round and appear in a lobular distribution, often surrounding a somewhat dilated duct with an apparent increase in the number of small glands compared to normal tissue.[2] Often, these two patterns are found in the same region, appearing to merge together (mixed lesions). The epithelium in both types of atrophy is composed of two layers consisting of flat basal

cells and cubical to low-columnar luminal cells. The majority of luminal cells in atrophic regions contain scant basophilic cytoplasm. The spatial relation between PIA and high-grade PIN or carcinoma was examined as previously described.[12] We recorded whether the atrophic lesion was merging directly with high-grade PIN, merging with carcinoma, adjacent to high-grade PIN and/or carcinoma (≤100 μm), near to high-grade PIN and/or carcinoma (>100 μm to ≤1 mm), and distant from high-grade PIN and/or carcinoma (>1 mm). We also evaluated the nuclear features of the PIA luminal cells and classified individual lesions as containing no nuclear atypia, or having focal atypia (<1% of atrophic cells) consisting of nucleolar and nuclear enlargement beyond that of normal epithelium, but less than that found in high-grade PIN. These regions containing nuclear atypia were designated as focal low-grade PIN, as indicated previously.[12] Nucleolar enlargement in atrophic cells directly abutting acute or chronic inflammatory cells was considered reactive atypia and not PIN.

Immunohistochemistry

Immunohistochemistry for high-molecular weight cytokeratin (HMWCK) and GSTP1 was performed with 34βE12 (primary monoclonal, dilution 1:50; Enzo Biochem, Farmingdale, NY) and anti-GSTP1 (rabbit polyclonal, 1:4000; DAKO, Carpinteria, CA) using the EnVision+ detection system (DAKO). Paraffin sections were deparaffinized and rehydrated through a graded alcohol series. Steam heating in citrate buffer (Vector Laboratories Inc., Burlingame, CA) was performed for 20 minutes for antigen retrieval. Primary antibodies were incubated either overnight at 4°C (GSTP1) or for 45 minutes at room temperature (34βE12). Slides were counterstained with hematoxylin.

Cell Culture

The established human prostate cancer cell line LNCaP (clone FGC, American Type Culture Collection catalog no. CRL-1740) with known *GSTP1* promoter hypermethylation,[27] obtained from the American Type Culture Collection (Rockville, MD), was grown in RPMI 1640 (Life Technologies, Inc., Gaithersburg, MD) and 10% fetal calf serum.

Laser Capture Microdissection

Two serial 10-μm sections were deparaffinized in two changes of xylene solutions for 5 minutes and rehydrated in 100%, 100%, and 95% ethanol for 3 minutes, 3 minutes, and 1 minute each, followed by staining with Hematoxylin 7211 (Richard-Allan Scientific, Kalamazoo, MI) for 45 seconds and Eosin-Y (Richard-Allan Scientific) for 1 second after rinsing with distilled water. The sections were dehydrated in 95%, 100%, and 100% ethanol for 1 minute each, followed by two changes of xylene for 5 minutes each and air-dried. Regions of normal epithelium, hyperplastic epithelium from transition zone nodules (BPH), PIA, high-grade PIN, and prostatic adenocarcinoma were obtained by LCM using the Pixcell II LCM system (Arcturus Engineering Inc., Mountain View, CA) from one or two sections using the CapSure HS LCM Caps (Arcturus Engineering Inc.). All prostates contained multiple regions of normal appearing epithelium and PIA, and many contained high-grade PIN and areas of nodular hyperplasia (BPH) in the transition zone. Regions of these histologies that were considered large enough to microdissect were selected at random. Carcinoma lesions were also multifocal in the prostates and these were also selected at random. To augment the resolution of the LCM in cases in which PIA and regions of high-grade PIN were in close proximity or merging, in many cases, slides were temporarily coverslipped and scanned using the BLISS System (Bacus Laboratory Inc., Lombard, IL). This produces a high-resolution map of the entire region of interest that can be used as a guide during LCM. After coverslips were removed, LCM was performed in conjunction with simultaneous visualization on a separate computer screen using the BLISS images. This allowed unambiguous isolation by LCM of atrophic cells from lesions where atrophy was merging with high-grade PIN or adenocarcinoma cells without isolation of high-grade PIN cells or adenocarcinoma cells. That the neoplastic cells were not procured in these cases was verified by microscopic examination and permanently recorded by rescanning the slides using the BLISS system after microdissection.

Isolation of Genomic DNA

DNA was isolated from the LNCaP cell line (positive control for *GSTP1* promoter hypermethylation) and hyperplastic tonsil gland (negative control) by use of a QIAamp DNA Mini Kit (Qiagen Inc., Valencia, CA) following the manufacturer's protocol. The concentrations of extracted DNA were measured with spectrometry. The cells captured with LCM were digested in 20 μl of proteinase K buffer (2 mg/ml proteinase K, 10 mmol/L Tris-HCl, pH 8.0, 0.1 mmol/L ethylenediaminetetraacetic acid, and 1% Tween 20) at 55°C overnight. After overnight incubation, the samples were incubated at 95°C for 8 minutes to inactivate the proteinase K. The DNA was isolated with standard phenol extraction and ethanol precipitation by adding 1.5 μl of glycogen (20 mg/ml; Roche Diagnostics Corp., Indianapolis, IN) as a carrier. The isolated DNA was eluted in 50 μl of H_2O.

To determine the starting amount of DNA for bisulfite modification, DNA extracted with LCM was quantified by use of real-time quantitative polymerase chain reaction (PCR) with SYBR Green I. Real-time quantitative PCR analyses were performed with the i-Cycler IQ Real-Time Detection System (Bio-Rad Laboratories, Inc., Hercules, CA). The concentration of DNA was measured using the absolute standard curve method following the i-Cycler IQ Real-Time Detection System Resource guide. An absolute standard curve was constructed with 10-fold serial dilutions of LNCaP DNA ranging from 50 ng to 5 pg using a human β-globin primer set. PCR primers of β-globin

Figure 1. Promoter region of the *GSTP1* gene. Two different primer sets targeting densely methylated alleles are depicted. Both primer sets have a common reverse primer.

were 5′-GCAACCTCAAACAGACACCA-3′ (forward) and 5′-CCTCACCACCAACTTCATCC-3′ (reverse). The quantitative PCR reaction was performed with 1.0 μl of DNA template in 25 μl of reaction mixture containing 2.5 μl of 10× PCR Buffer (Roche Applied Biosystems, Branchburg, NJ), 200 μmol/L each of the four dNTPs, 3.0 mmol/L $MgCl_2$, 0.4 μmol/L each forward and reverse primer, 0.5 μl of 1:2000 dilution SYBR Green I (10,000× stock) (Molecular Probes Inc., Eugene, OR) and 1.25 U of Ampli *Taq* Gold (Roche Applied Biosystems). PCR reactions were performed in triplicate. The PCR reaction was subjected to hot start at 95°C for 10 minutes followed by 45 cycles of denaturation at 95°C for 15 seconds, annealing, and extension at 65°C for 30 minutes. DNA amplifications were performed in a 96-well reaction plate.

Methylation-Specific PCR (MSP)

In the majority of isolated specimens, 10 ng of genomic DNA, measured with real-time PCR, was modified with bisulfite using the CpGenome DNA modification kit (Intergen, Norcross, GA) following the manufacturer's protocol. The bisulfite-modified DNA was eluted in 25 μl of H_2O. In some LCM samples where yields were lower, between 1.9 and 10 ng of DNA was treated with bisulfite. To enhance the sensitivity of detection of methylated alleles, two different primer sets were used for MSP. The first set[34] utilizes two sets of primers for each sample; one that detects densely methylated alleles (a) and the other that detects unmethylated alleles (b). The second set[28] utilizes two sets of primers as well; one that detects densely methylated alleles (c) and the other that detects an unrelated gene, MYOD1, that controls for efficacy of bisulfite conversion (d). a, GSTP1-methylated specific primer 1, 5′-TTCGGGGTGTAGCGGTCGTC-3′ (forward), 5′-GCCCCAATACTAAATCACGACG-3′ (reverse); b, GSTP1 unmethylated specific primer, 5′-GATGTTTGGGGTGTAGTGGTTGTT-3′ (forward), 5′-CCACCCCAATACTAAATCACAACA-3′ (reverse); c, GSTP1 methylated specific primer 2, 5′-AGTTGCGCGGCGATTTC-3′ (forward), 5′-GCCCCAATACTAAATCACGACG-3′ (reverse); d, MYOD1 primer, 5′-CCAACTCCAAATCCCCTCTCTAT-3′ (forward), 5′-TGATTAATTTAGATTGGGTTTAGAGAAGGA-3′ (reverse). The two primer sets to detect densely methylated alleles in the human *GSPT1* promoter are depicted in Figure 1. The PCR reaction was performed with 2.5 μl of bisulfite-modified DNA template in 25 μl of reaction mixture containing 2.5 μl 10× PCR buffer, 200 μmol/L of each dNTP, 3.0 mmol/L $MgCl_2$ (a, b), 3.5 mmol/L $MgCl_2$ (c), 4.5 mmol/L $MgCl_2$ (d), 0.25 μmol/L each primer (a, b), 0.6 μmol/L each primer (c, d), and 1.25 U of Ampli *Taq* Gold. The PCR reaction was subjected to hot start at 95°C for 10 minutes followed by 50 cycles of denaturation at 95°C for 1 minute, annealing at 59°C for 30 seconds, and extension at 72°C for 1 minute and a final extension at 72°C for 7 minutes (a, b), or 50 cycles of denaturation at 95°C for 15 seconds, annealing, and extension at 65°C for 1 minute and a final extension at 72°C for 7 minutes (c, d). Eight μl of each PCR reaction were loaded onto a 3% agarose gel and stained with Gel Star nucleic acid gel stain (BMA Bio Whittaker Molecular Applications, Rockland, ME). DNA from the prostate cancer cell line LNCaP, which is known to contain only densely methylated GSPT1 alleles,[16] was used as a positive control for GSTP1 methylation, normal human tonsil DNA was used as a negative control, and dH_20 used as a control for contamination in PCR reactions.

The Sensitivity of MSP for the GSTP1 CpG Island

Although MSP is a very sensitive method for detecting methylation changes, bisulfite treatment can result in decreased yields of DNA. We found that to consistently obtain the correct PCR products, ~1 ng of LNCaP DNA was needed for bisulfite modification. The results of real-time quantitative PCR with the β-globin primers showed ~5 to 10 pg of genomic DNA was obtained from one cell, such that 1000 to 2000 cells were needed to obtain 10 ng of genomic DNA. In an experiment to investigate the sensitivity of MSP, LNCaP DNA was mixed with tonsil DNA in different proportions, and the limit of detection was 1% of LNCaP DNA (100 pg) in a total of 10 ng of bisulfite-treated DNA for both primer sets (data not shown).

Statistical Analysis

Differences in frequency of *GSTP1* hypermethylation between normal and hyperplastic epithelium, PIA, high-grade PIN, and adenocarcinoma were assessed with the Fisher's exact or the chi-square test using Stata 6.0 for Microsoft Windows software.

Results

Histological and Key Immunophenotypic Features of PIA

The histological features of PIA have been described (see Materials and Methods).[2,4] The histological classifications of the microdissected PIA lesions are shown in Table 1. An example of PIA is shown in Figure 2, a stereotypic case in which a large fraction of the peripheral zone was occupied by atrophic epithelium classified as simple atrophy. Of the 64 PIA lesions microdissected, 44 (68.8%) were classified as simple atrophy, 5 (7.8%) as postatrophic hyperplasia (PAH), and 15 (23.4%) as mixed simple atrophy and postatrophic hyperplasia.

PIA can also be recognized and delineated by immunohistochemical staining using the 34βE12 antibody. Although 34βE12 staining is typically restricted to basal

Table 1. Histological Features and Methylation Status of PIA Lesions

Pt no.	Lesion no.	Type of PIA	Primer 1	Primer 2	Relation to HGPIN	Relation to CaP	LGPIN
1	1	SA/PAH	□	□	M	D	−
1	2	SA	□	□	M	D	+
1	3	SA	□	□	D	D	−
1	4	SA	□	□	N	D	−
2	1	SA	□	□	N	D	−
2	2	SA	□	□	D	D	−
2	3	SA	□	□	D	D	−
3	1	SA	□	□	M	D	+
3	2	SA	□	□	D	D	−
3	3	PAH	□	−	D	N	−
4	1	SA	−	□	D	D	+
5	1	SA	□	□	D	D	−
5	2	SA	□	□	D	N	−
6	1	SA	□	□	D	N	+
7	1	SA	□	□	D	D	−
7	2	SA	−	□	D	A	−
8	1	SA	−	□	M	D	−
8	2	SA/PAH	□	□	N	D	−
8	3	SA	□	□	D	D	−
9	1	SA	□	−	M	D	+
9	2	SA	□	−	D	A	−
9	3	SA	□	−	M	D	+
10	1	SA	□	□	D	N	+
10	2	PAH	□	□	M	D	−
11	1	SA	□	□	M	D	+
12	1	SA/PAH	□	□	D	D	−
12	2	SA	□	−	N	N	−
13	1	SA	□	□	M	D	+
13	2	PAH	□	□	D	D	−
13	3	SA	□	□	N	A	+
14	1	SA	□	□	D	D	−
14	2	SA	−	□	N	D	−
14	3	SA	■	□	N	D	−
14	4	SA	□	□	M	N	+
15	1	SA/PAH	□	□	D	D	+
15	2	SA/PAH	□	□	D	D	−
16	1	SA/PAH	□	□	D	D	−
16	2	SA	□	■	D	D	+
16	3	SA/PAH	□	□	D	M	+
17	1	SA/PAH	□	□	M	D	−
17	2	SA	□	□	M	D	+
18	1	SA	□	−	D	D	−
18	2	SA	□	□	D	D	−
19	1	SA/PAH	□	□	D	A	−
19	2	SA/PAH	□	□	M	D	+
19	3	SA	□	□	D	D	−
20	1	PAH	□	□	D	D	−
20	2	SA	□	□	D	D	−
20	3	SA/PAH	□	□	D	D	−
20	4	SA/PAH	□	−	D	D	−
21	1	SA	□	−	D	D	−
21	2	PAH	□	□	D	D	−
22	1	SA	−	□	D	D	−
22	2	SA/PAH	□	□	D	D	−
23	1	SA	□	□	D	D	+
23	2	SA/PAH	−	□	M	M	+
24	1	SA	□	□	N	D	−
24	2	SA	■	■	D	D	−
25	1	SA	□	□	D	N	−
25	2	SA	□	■	M	D	+
26	1	SA	□	□	M	D	−
26	2	SA	−	□	D	N	+
27	1	SA/PAH	□	□	N	N	−
27	2	SA	□	□	D	N	−

GSTP1 primers: filled boxes, methylated results; open boxes, unmethylated results; dash, not amplified with control primer. Relationship to high-grade PIN (HGPIN) or prostatic adenocarcinoma: M, merging; A, adjacent; N, near; D, distant. LGPIN: +, containing focal prominent nucleoli in atrophic cells (low-grade PIN); −, no low-grade PIN present in lesion dissected.

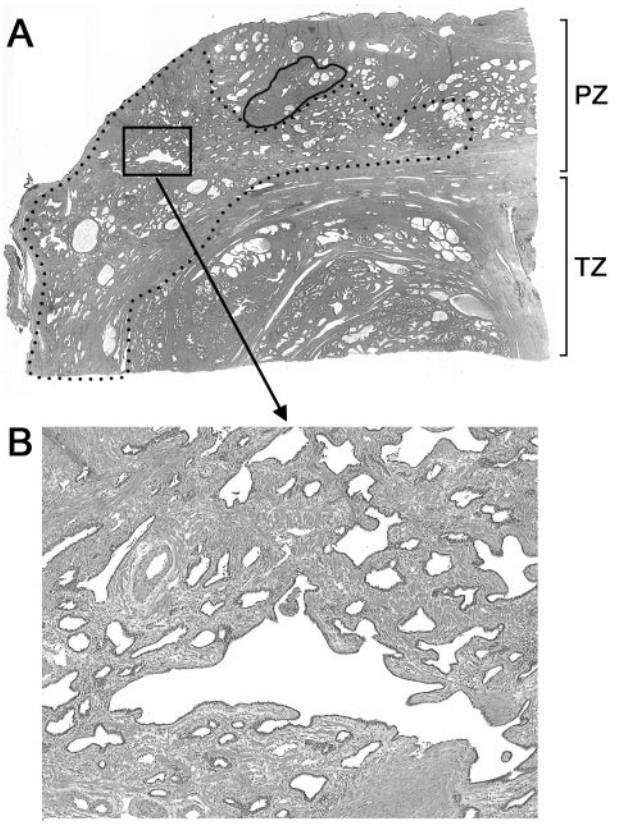

Figure 2. Histology of PIA of the prostate. **A:** Low-power view of PIA (**dotted lined area**) occurring adjacent to adenocarcinoma (**outlined area**) occupied a very large percentage of the total peripheral zone (PZ). A hyperplasia nodule (BPH) is seen in transitional zone (TZ). **B:** Intermediate-power view of **boxed area**. This lesion was classified as simple atrophy (SA). Original magnifications: ×12.5 (**A**); ×40 (**B**).

cells in normal appearing prostate epithelium, we have shown that it is elevated in many of the atrophic luminal cells of PIA if steam heat, and not protease digestion, is used for antigen retrieval.[35] Figure 3 shows an example of this staining in another typical simple atrophy lesion. Another characteristic immunohistochemical feature of PIA is that GSTP1 protein is also elevated in many, but not all, of the luminal cells (Figure 3).

As previously noted,[4,12] a fraction of PIA lesions (16 of 64, 25%) contained areas that merged with high-grade PIN (Table 1), the latter being characterized by cells with numerous prominent nucleoli (between 1.5 and 2.5 μm as measured by the BLISS system). Most of these cases also contained atrophic appearing cells containing somewhat more cytoplasm with nuclear and nucleolar enlargement that was intermediate between normal epithelium and high-grade PIN epithelium, suggestive of transitions between PIA and high-grade PIN.[12] PIA was near to high-grade PIN in 9 lesions (14.1%), and distant from high-grade PIN in 39 lesions (60.9%). Of the 48 PIA lesions where there was no apparent merging with high-grade PIN, 9 contained low-grade PIN (Figure 4). Careful LCM permitted the selective isolation of atrophic cells, even atrophic cells merging directly with high-grade PIN or adenocarcinoma, without contamination by PIN or adenocarcinoma cells (Figure 5). To further avoid the possibility of contamination, during microdissection we also carefully avoided cells in PIA containing any nucleolar enlargement when the lesion was merging with high-grade PIN.

Although we did not find merging between PIA and adenocarcinoma in a previous study,[12] there was evidence of PIA merging with adenocarcinoma in 2 of 64 lesions (3.1%) in the present study (Figure 6). PIA was adjacent to adenocarcinoma in 4 lesions (6.3%), near to adenocarcinoma in 10 lesions (15.6%), and distant from adenocarcinoma in 48 lesions (75.0%). Inflammatory infiltrates were found in all microdissected areas. The extent of inflammation varied from mild chronic to moderate acute inflammation, although the majority of cases contained mild to moderate amounts of chronic inflammation and mild or no acute inflammation.

GSTP1 CpG Island Hypermethylation

To assess the amount of isolated genomic DNA templates obtained by LCM, we used an aliquot of each sample obtained by LCM for real-time PCR. In a typical LCM session, we obtained ~1000 to 3000 cells from each of two adjacent slides. An example of a lesion before and after LCM is shown in Figure 5. The yield of amplifiable template genomic DNA ranged from 1.95 ng to 54.0 ng. One hundred ninety-nine of the 200 (99.5%) samples showed readily amplifiable DNA using either set of primers after bisulfite treatment. Bisulfite-modified DNA was successfully amplified in 178 of the 200 samples (89%) using the first primer set (GSPT1 methylated primer 1 and unmethylated primer) and in 177 of the 200 samples (88.5%) using the second primer set (GSTP1 methylated primer 2 and MYOD primer). One hundred fifty-six of the 200 lesions (78%) amplified for both primer sets. A summary of the results of MSP is shown in Table 2. Two examples of MSP analysis are shown in Figure 7.

GSTP1 promoter hypermethylation was not detected in normal epithelium ($n = 48$) from 27 patients or in hyperplastic epithelium (BPH) ($n = 22$) from 20 patients, despite the fact that methylation was uniformly detected in the positive control bisulfite-treated DNA from the LNCaP cell line in these experimental runs (Table 2).

GSTP1 promoter methylation was found in 4 of 64 PIA lesions (6.3%) from 4 of 27 patients (14.8%). One lesion demonstrated methylated alleles using primer set 1, two lesions contained methylated alleles using primer set 2, and one lesion had detectable methylation using both primer sets 1 and 2. All four methylated PIA lesions were considered simple atrophy. Two of four microdissected lesions with methylated alleles contained focal markedly atypical cells (low-grade PIN). Although one of the four methylated atrophy lesions merged with high-grade PIN, the other three lesions did not and none of the positive lesions either merged with cancer or were directly adjacent to cancer.

For statistical analysis, we pooled the results from the normal epithelium ($n = 48$) with that of hyperplastic epithelium (BPH) ($n = 22$) to obtain a total of 70 benign nonatrophic epithelial regions. Comparing the benign

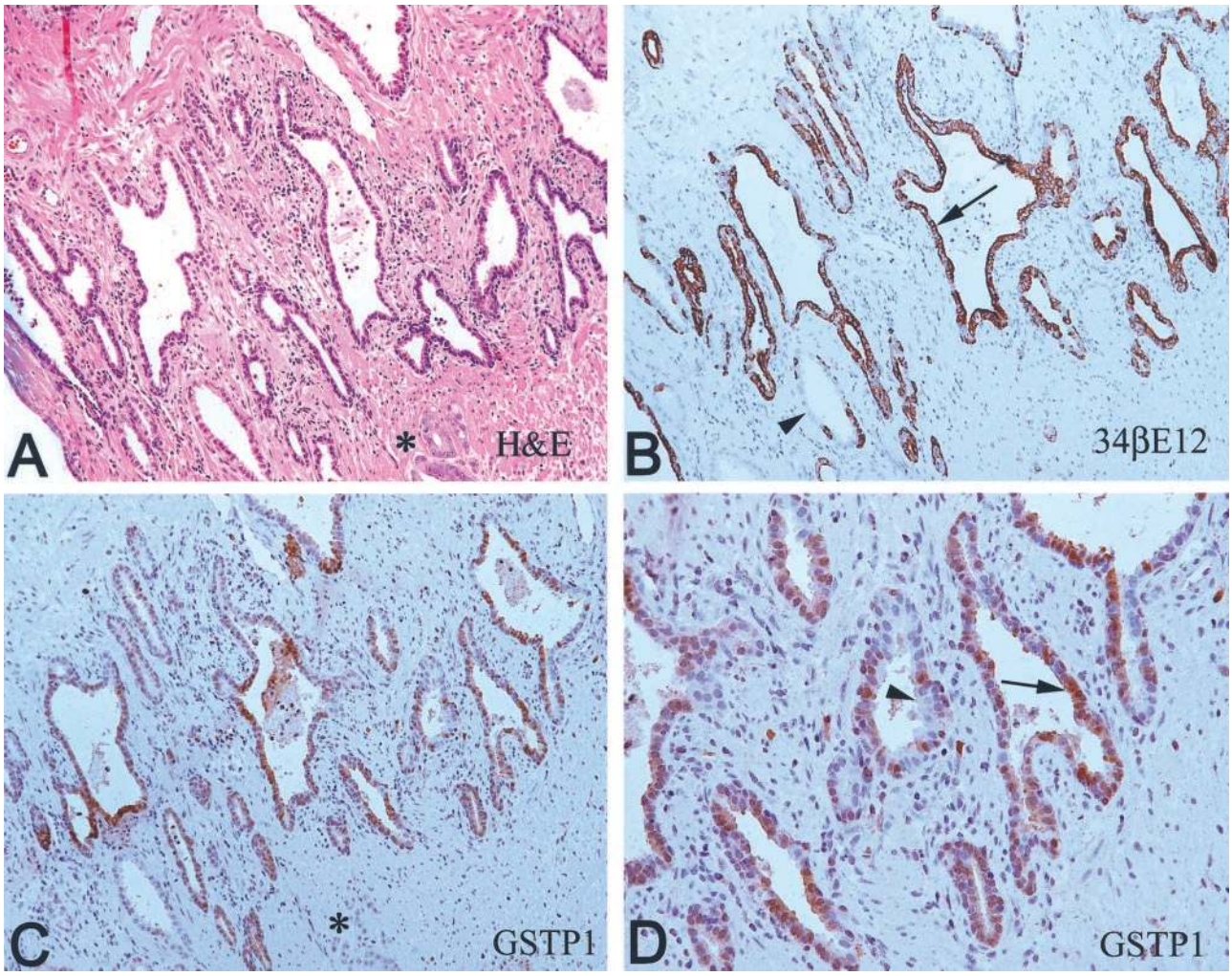

Figure 3. Immunohistochemical features of PIA. **A:** Medium-power view of PIA stained with H&E. **Asterisk** indicates adenocarcinoma. **B:** Medium-power view of PIA stained with the 34βE12 monoclonal antibody. **C:** Heterogeneity of expression of GSTP1 in PIA. **D:** Higher power view of area in part of **C**. In parts **B** and **D**, **arrows** indicate positive epithelial cells in PIA, and **arrowheads** indicate PIA cells with no staining. Original magnifications: ×100 (**A–C**); ×200 (**D**).

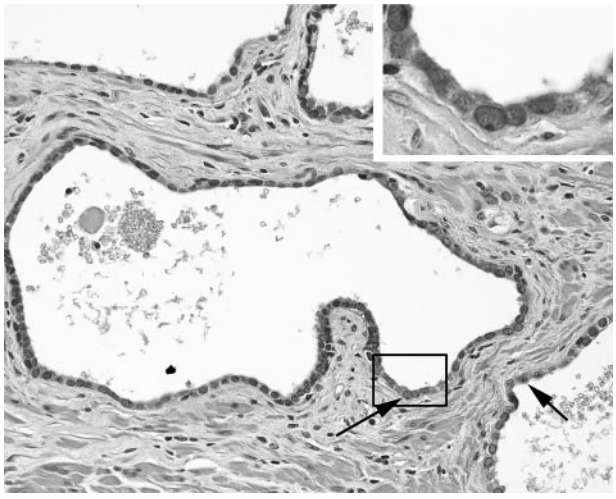

Figure 4. Atrophic gland showing features of low-grade PIN. Region of PIA showing scattered cells with slight nuclear enlargement and prominent nucleoli (**arrows**) designated as PIA containing focal low-grade PIN. Original magnifications: ×200; ×600 (**inset**).

and hyperplastic epithelium (0 of 70) to that of PIA (4 of 64), there was a statistically significant difference in the frequency of *GSTP1* promoter hypermethylation (P = 0.049, Fisher's exact test) (Table 2).

Hypermethylation of the *GSTP1* promoter was detected in 13 of 27 high-grade PIN lesions (48.1%) using the first primer set and 16 of 29 lesions (55.2%) using the second primer set. Combined, 22 of 32 high-grade PIN lesions (68.8%) contained methylated alleles from 17 of 23 patients (73.9%). A statistically significant difference in the frequency of *GSTP1* promoter hypermethylation was found between PIA foci and high-grade PIN foci ($P <$ 0.001, chi-square) (Table 2).

Hypermethylation of the *GSTP1* promoter was detected in 23 of 30 adenocarcinoma lesions (76.7%) using the first primer set, and 25 of 31 lesions (80.6%) using second primer set. Combined, therefore, 30 of 33 carcinoma lesions (90.9%) contained methylated alleles. All 27 patients (100%) showed methylation in either of the two different methylated primer sites or both sites. There was a significant difference from high-grade PIN lesions to adenocarcinoma lesions (P = 0.03, chi-square) (Table 2).

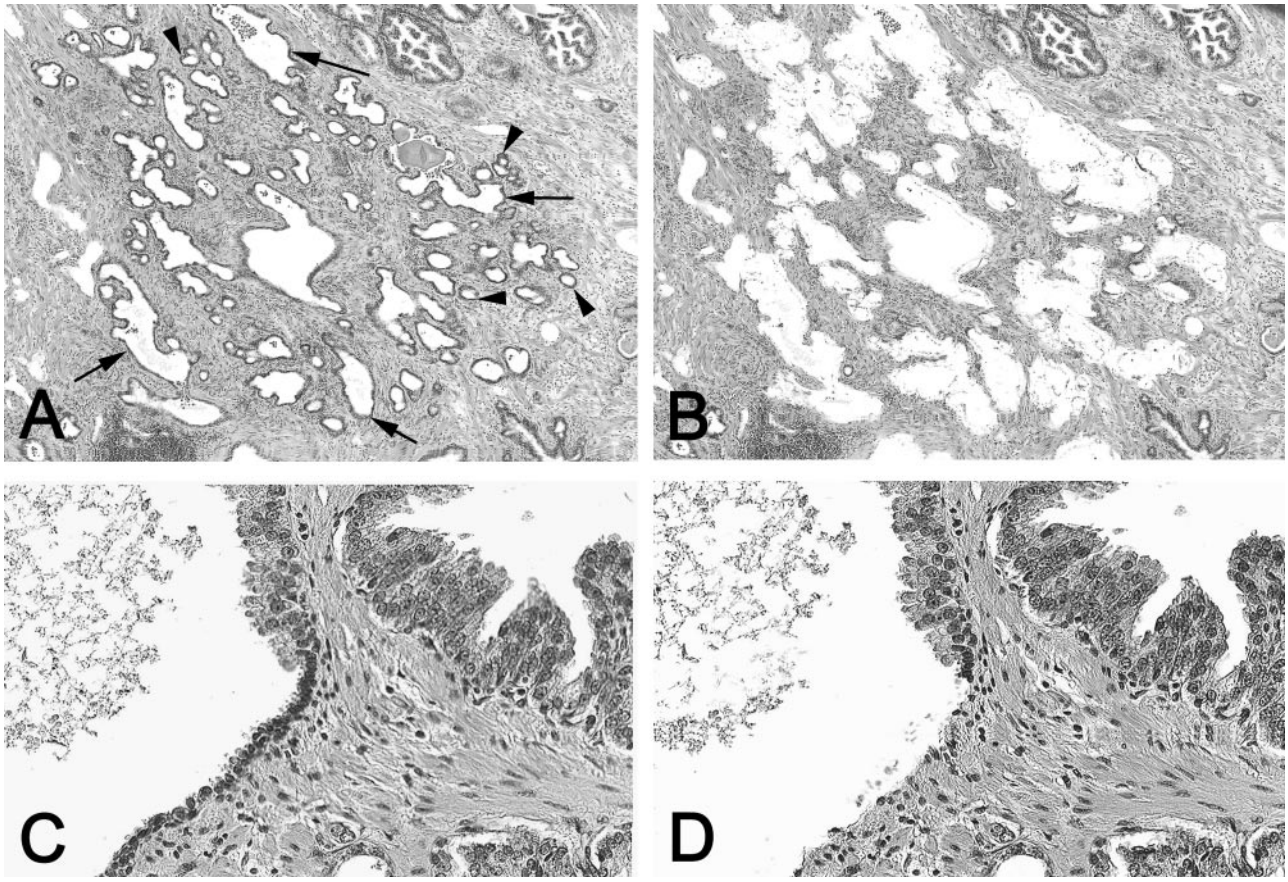

Figure 5. Example of tissue sections scanned with the BLISS system before and after LCM. **A–D:** Mixed simple atrophy and postatrophic hyperplasia lesion from a representative case was successfully microdissected where the same slide was scanned before and after microdissection using the BLISS system. **Arrows** indicate large acini classified as simple atrophy and **arrowheads** indicate small round acini classified as postatrophic hyperplasia. **C** and **D:** A separate case showing areas of atrophic epithelium merging directly with epithelium containing more cytoplasm and nuclear atypia (high-grade PIN). Note in **D** that high-grade PIN cells have not been procured. Original magnifications: ×25 [**A** (before LCM), **B** (after LCM)]; ×200 [**C** (before LCM), **D** (after LCM)].

The ability of a given DNA sample to be amplified by both primer sets, as opposed to a single primer set, may be a measure of the density of methylation of the GSTP1 promoter. The ratio of lesions that contained methylation changes in both primer sites to lesions that showed methylation change in either set of primers was 1 of 4 PIA lesions (25.0%), 7of 18 high-grade PIN lesions (38.9%), and 18 of 27 adenocarcinoma lesions (66.7%).

Discussion

In this study we report results of the first attempt to examine the methylation status of the CpG island in the *GSTP1* promoter region using microdissected samples. We found that a small subset of PIA lesions (6.3%) in the human prostate contains detectable hypermethylation of this region. Consistent with previous studies using non-microdissected samples,[16,33] we found that the majority of areas of carcinoma (90.9%) and the majority of high-grade PIN frequently (68.8%) contained this molecular alteration, but that normal appearing epithelium and hyperplastic epithelium did not (0%).

In a previous study examining the topographic relation of PIA to high-grade PIN and adenocarcinoma, we selected 13 radical prostatectomy specimens that contained on average 5 separate foci of carcinoma and 50 separate foci of high-grade PIN.[12] To study the earliest lesions, these prostates all had tumor volumes of less than 0.5 cm^3. Although 42% of high-grade PIN lesions were found to merge directly with atrophic epithelium, no carcinomas were found to merge directly with atrophic epithelium.[12] However, 88% of carcinoma lesions were within 1 mm of PIA.[12] Previous studies by others using H&E-stained slides did report areas of atrophy that appeared to be merging directly with carcinoma,[10,11] and in the present study two PIA lesions appeared to be directly merging with small foci of adenocarcinoma. Twenty-five percent of the PIA lesions were found to merge directly with high-grade PIN and 31.3% of the PIA lesions contained at least some cells with prominent nucleoli (low-grade PIN). Thus, morphological evidence indicates that atrophic epithelial cells can develop nuclear atypia and architectural changes that proceed either to PIN or to carcinoma directly. Morphological data alone, however, cannot be used to directly implicate a cancer precursor. Thus, several groups have begun to subject prostate atrophy to molecular analysis. Previous studies have indicated that chromosome 8 abnormalities, which are common in prostate adenocarcinoma, were found in areas of simple atrophy and postatrophic hyperplasia. Gain of chromosome 8

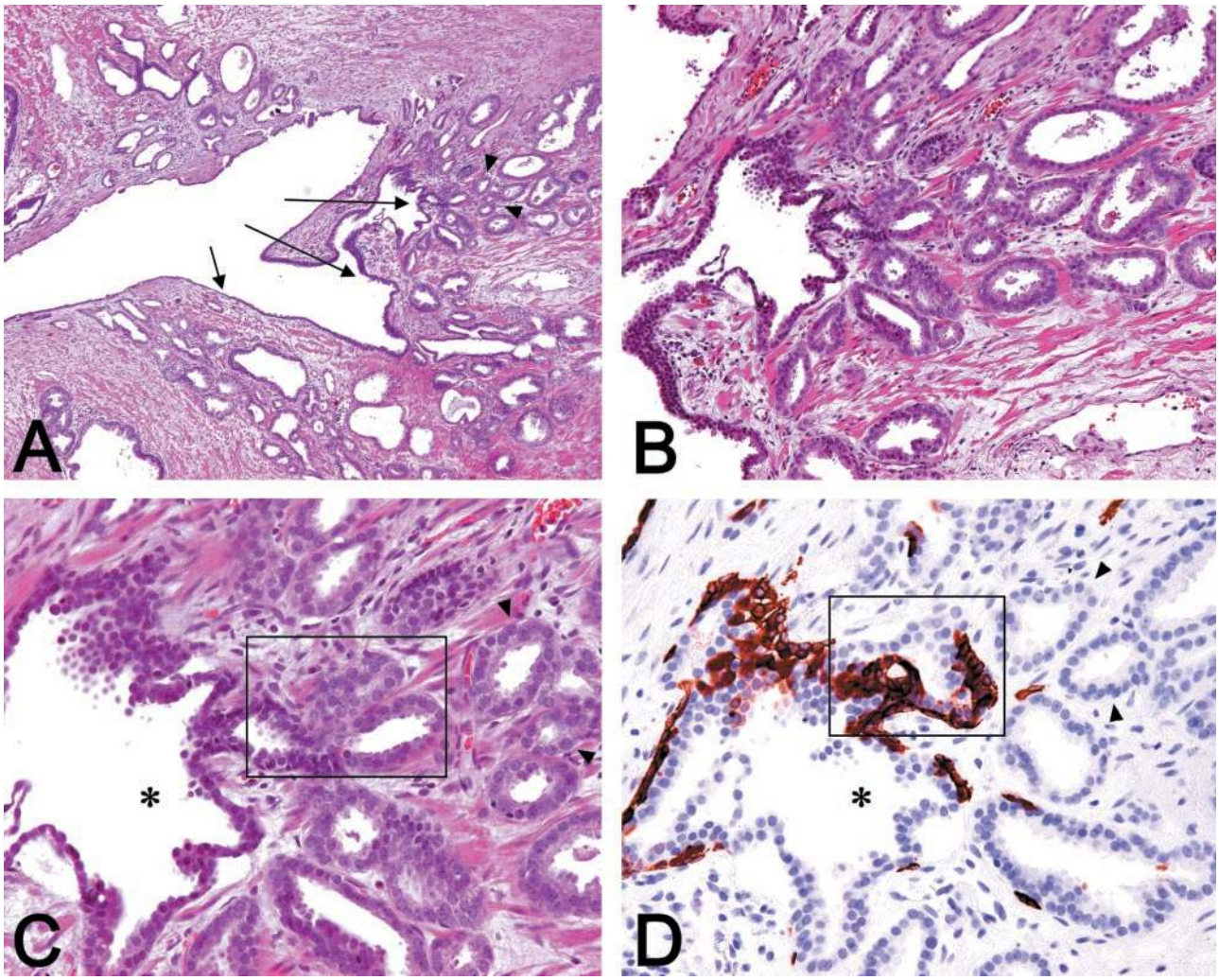

Figure 6. PIA merging with adenocarcinoma (CaP). **A:** Low-power view of a focus of PIA apparently merging with prostatic adenocarcinoma stained with H&E. **Arrows** indicate PIA lesion. **Arrowheads** indicate adenocarcinoma acini. **B:** Medium-power view of area in **A**. **C:** High-power view. **D:** High-power view of region of atrophy apparently merging with adenocarcinoma stained with the 34βE12 monoclonal antibody. **Arrowheads** indicate adenocarcinoma acini. **Asterisks** indicate the lumen of atrophic acinus. Original magnifications: ×40 (**A**); ×100 (**B**); ×400 (**C**, **D**).

centromere sequences was noted in 1.3% of normal, 2.1% of simple atrophy, 2.8% of high-grade PIN, 4.0% of postatrophic hyperplasia, and 6.0% of adenocarcinoma.[13] In a study of postatrophic hyperplasia from Japan, Tsujimoto and colleagues[14] reported that 5.3% of atrophy lesions, 4.2% of high-grade PIN, and 25.0% of adenocarcinoma contained at least some cells harboring p53 mutations. Thus together with our results, there is accumulating evidence that a subset of focal atrophy lesions in the prostate may contain somatic molecular alterations characteristic of prostate cancer.

Table 2. Hypermethylation in *GSTP1* CpG Island in Normal Epithelium, BPH, PIA, High-Grade PIN, and Adenocarcinoma in the Prostate

	n (patients)	Any *GSTP1* methylation* (*n*, areas)
Normal	27	0/48 (0.0%)
BPH	20	0/22 (0.0%)
PIA	27	4/64 (6.3%)†
HGPIN	23	22/32 (68.8%)††
CaP	27	30/33 (90.9%)†††

*, Shown are number of microdissected regions with any GSPT1 hypermethylation by either primer set divided by the total number of microdissected areas. †, $P = 0.049$ (Fisher's exact test) compared with the total of normal and BPH. ††, $P < 0.001$ compared with PIA (Fisher's exact test); †††, $P = 0.03$ compared with high-grade PIN (Chi-square test).

GSTP1 is a phase II detoxification enzyme that defends cells against DNA damage mediated by oxidants or electrophiles.[36] *GSTP1* may function as a caretaker gene, which when inactivated leads to additional somatic genome alterations that promote tumor growth.[37] For example, mice with disrupted *GSTP1/2* alleles showed an increase in skin tumorigenesis in response to topical carcinogen treatment.[38] Rats fed 2-amino-1-methyl-6-phenylimidazo [4,5-β] pyridine (PhIP), which is the most abundant of the mutagenic heterocyclic amines found in well-done or charred meats,[39] showed mutations in prostate DNA and developed prostate carcinoma.[40,41] Loss of GSTP1 function was found to increase PhIP induced DNA damage in human prostate cells exposed to metabolically activated PhIP *in vitro*.[42]

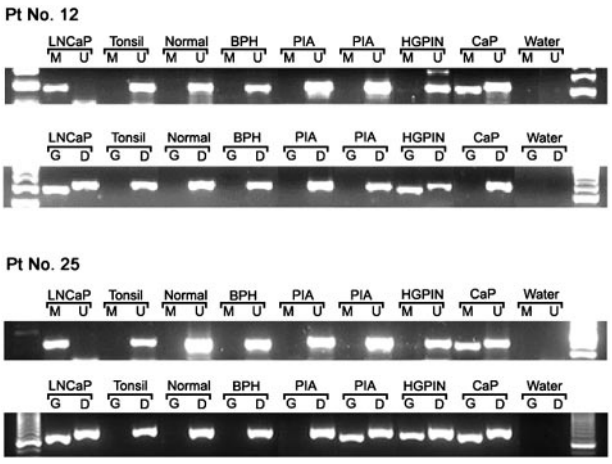

Figure 7. MSP of *GSTP1* in prostate tissues. The tumor cell line LNCaP as a positive control for *GSTP1* methylation, normal human tonsil DNA as a negative control, and a water control for contamination in the PCR reaction are indicated. DNA size markers are present at the ends of each gel. Lanes designated M, amplified products with *GSTP1*-methylated primer 1; lanes designated U, amplified products with *GSTP1* unmethylated primer; lanes designated G, amplified products with *GSTP1*-methylated primer 2; lanes designated D, amplified product with MYOD1 primer. **Top:** The two panels are from patient 12 where microdissected tissues were obtained from areas of normal, BPH, PIA (two separate lesions), high-grade PIN (HGPIN), and adenocarcinoma (CaP). The cancer lesion (CaP) from patient 12 shows methylation with methylated primer set 1 and the high-grade PIN (HGPIN) lesion from patient 12 shows methylation with methylated primer set 2. Other tissues from patient 12 showed no evidence of methylation with either primer set. **Bottom:** The two panels are from patient 25. In the **top** portion, methylation was detected in the CaP lesion, and in the **bottom** portion, methylation was detected in the second PIA lesion as well as the HGPIN and CaP lesions. Only the cancer lesion in patient 25 showed methylation with both primer sets.

In human prostates, the majority of high-grade PIN and almost all adenocarcinoma cells fail to express GSTP1. This lack of protein expression is associated with hypermethylation of the *GSTP1* CpG island encompassing its 5′ upstream promoter region.[27,33] Although the normal luminal cells generally do not express GSTP1, strong staining is seen in underlying basal cells. We have proposed that the consistent expression of GSTP1 may protect basal cells from DNA damage.[17] In contrast, in addition to the basal cells, many of the luminal cells in PIA lesions stain positively for GSTP1. We hypothesized that the cells in PIA that lack GSTP1 expression may be a consequence of *GSTP1* CpG island hypermethylation. The data presented here demonstrate that *GSTP1* CpG island hypermethylation changes occur in some PIA lesions. These results provide further molecular evidence that at least some PIA lesions may harbor cells already initiated to progress to high-grade PIN and/or prostatic adenocarcinoma. The fact that only 6.3% of focal atrophy lesions contain methylated *GSTP1* alleles does not preclude PIA from being a major precursor to prostate cancer because atrophy can occupy a very large percentage of the total peripheral zone of the prostate (Figure 2).[10] Therefore, if 6.3% of prostate atrophy regions can potentially lead to carcinoma, then the very high prevalence and extent of atrophy may help explain the high frequency of multifocal prostate cancer and high-grade PIN. It would be of interest to repeat this study in different patient populations from different geographic locations to determine how widespread these findings are.

Our results differ somewhat from that of Jeronimo and colleagues.[28] In their study, hypermethylation of the *GSTP1* CpG island was identified in 29% of BPH samples whereas none of the BPH samples in our study showed *GSTP1* hypermethylation. There are several potential explanations for this discrepancy. First, Jeronimo and colleagues[28] used a much larger amount of DNA for MSP. Thus, the chance of finding rare methylated cells in BPH tissue was increased in their study. Another possible explanation is that BPH samples in patients treated for BPH symptoms, such as those used by Jeronimo and colleagues,[28] may be biologically different from those samples obtained from an enlarged transition zone containing histological nodular hyperplasia, as used in the present study. Finally, Jeronimo and colleagues[28] did not use microdissected samples, and it is possible that some of their specimens contained occult carcinoma or PIN. Consistent with our results, however, they did find quantitatively much less GSTP1 hypermethylation in BPH than in cancer specimens.[28]

The results of MSP using two different primer sets support the hypothesis that the methylation of individual CpG sites in the island may gradually increase during progression of the neoplastic process. If so, inhibition of *de novo* methylation at any stage could be important for prevention of cancer development.

Although these studies provide new additional evidence that some foci of prostate atrophy may be at risk for developing into true neoplastic lesions, many new questions are raised by these results. What cells in PIA have *GSTP1* hypermethylation? We presume that cells that express GSTP1 in PIA would not have dense CpG island methylation. This question may best be addressed in the future by *in situ* methods for detection of CpG island hypermethylation[43] combined with immunostaining for GSTP1 protein. Another possibility is that a higher percentage of PIA lesions contain a small number of cells with methylated *GSTP1* alleles but that this small fraction may not be routinely detected by our method. Another question is: does the extent of methylation changes at the *GSTP1* CpG island increase with neoplastic transformation in the prostate? Finally, does immune-mediated oxidant stress lead to aberrant methylation changes? Further studies are needed to address these issues.

In summary, *GSTP1* CpG island hypermethylation appeared in a subset of PIA lesions, though no *GSTP1* hypermethylation was identified in normal appearing epithelium or epithelium of BPH tissue. High-grade PIN and adenocarcinoma very frequently showed this somatic molecular alteration. Our data support the hypothesis that atrophic epithelium in a subset of PIA lesions may lead to high-grade PIN and/or adenocarcinoma. Because these lesions are so prevalent and extensive, even though only a small subset contain this key somatic DNA alteration, the clinical impact may be highly significant.

Acknowledgments

We thank Alan K. Meeker for careful reading of the manuscript, Helen Fedor and Marcella Southerland for prepar-

ing prostate tissues, Gerrun March for help with scanning images with BLISS system, and Elizabeth A. Saria for helpful discussions on real-time PCR analysis.

References

1. Putzi MJ, De Marzo AM: Prostate pathology: histologic and molecular perspectives. Hematol Oncol Clin North Am 2001, 15:407–421
2. Ruska KM, Sauvageot J, Epstein JI: Histology and cellular kinetics of prostatic atrophy. Am J Surg Pathol 1998, 22:1073–1077
3. McNeal JE: Normal histology of the prostate. Am J Surg Pathol 1988, 12:619–633
4. De Marzo AM, Marchi VL, Epstein JI, Nelson WG: Proliferative inflammatory atrophy of the prostate: implications for prostatic carcinogenesis. Am J Pathol 1999, 155:1985–1992
5. Ames BN, Gold LS, Willett WC: The causes and prevention of cancer. Proc Natl Acad Sci USA 1995, 92:5258–5265
6. Parsons JK, Nelson CP, Gage WR, Nelson WG, Kensler TW, De Marzo AM: GSTA1 expression in normal, preneoplastic, and neoplastic human prostate tissue. Prostate 2001, 49:30–37
7. Zha S, Gage WR, Sauvageot J, Saria EA, Putzi MJ, Ewing CM, Faith DA, Nelson WG, De Marzo AM, Isaacs WB: Cyclooxygenase-2 is up-regulated in proliferative inflammatory atrophy of the prostate, but not in prostate carcinoma. Cancer Res 2001, 61:8617–8623
8. Moore RA: The evolution and involution of the prostate gland. Am J Pathol 1936, 12:599–624
9. Rich AR: On the frequency of occurrence of occult carcinoma of the prostate. J Urol 1934, 33:215–223
10. Franks L: Atrophy and hyperplasia in the prostate cancer. Am J Pathol Bacteriol 1954, 68:617–621
11. Liavag I: Atrophy and regeneration in the pathogenesis of prostatic carcinoma. Acta Pathol Microbiol Scand 1968, 73:338–350
12. Putzi MJ, De Marzo AM: Morphologic transitions between proliferative inflammatory atrophy and high-grade prostatic intraepithelial neoplasia. Urology 2000, 56:828–832
13. Shah R, Mucci NR, Amin A, Macoska JA, Rubin MA: Postatrophic hyperplasia of the prostate gland: neoplastic precursor or innocent bystander? Am J Pathol 2001, 158:1767–1773
14. Tsujimoto Y, Takayama H, Nonomura N, Okuyama A, Aozasa K: Postatrophic hyperplasia of the prostate in Japan: histologic and immunohistochemical features and p53 gene mutation analysis. Prostate 2002, 52:279–287
15. Macoska JA, Trybus TM, Wojno KJ: 8p22 loss concurrent with 8c gain is associated with poor outcome in prostate cancer. Urology 2000, 55:776–782
16. Lee WH, Morton RA, Epstein JI, Brooks JD, Campbell PA, Bova GS, Hsieh WS, Isaacs WB, Nelson WG: Cytidine methylation of regulatory sequences near the pi-class glutathione S-transferase gene accompanies human prostatic carcinogenesis. Proc Natl Acad Sci USA 1994, 91:11733–11737
17. De Marzo AM, Coffey DS, Nelson WG: New concepts in tissue specificity for prostate cancer and benign prostatic hyperplasia. Urology 1999, 53:29–42
18. Neslon WG: The molecular pathogenesis of prostate cancer: a new role for inflammation. N Engl J Med 2003, 399:366–381
19. Lee WH, Isaacs WB, Bova GS, Nelson WG: CG island methylation changes near the GSTP1 gene in prostatic carcinoma cells detected using the polymerase chain reaction: a new prostate cancer biomarker. Cancer Epidemiol Biomarkers Prev 1997, 6:443–450
20. Millar DS, Ow KK, Paul CL, Russell PJ, Molloy PL, Clark SJ: Detailed methylation analysis of the glutathione S-transferase pi (GSTP1) gene in prostate cancer. Oncogene 1999, 18:1313–1324
21. Santourlidis S, Florl A, Ackermann R, Wirtz HC, Schulz WA: High frequency of alterations in DNA methylation in adenocarcinoma of the prostate. Prostate 1999, 39:166–174
22. Suh CI, Shanafelt T, May DJ, Shroyer KR, Bobak JB, Crawford ED, Miller GJ, Markham N, Glode LM: Comparison of telomerase activity and GSTP1 promoter methylation in ejaculate as potential screening tests for prostate cancer. Mol Cell Probes 2000, 14:211–217
23. Goessl C, Krause H, Muller M, Heicappell R, Schrader M, Sachsinger J, Miller K: Fluorescent methylation-specific polymerase chain reaction for DNA-based detection of prostate cancer in bodily fluids. Cancer Res 2000, 60:5941–5945
24. Goessl C, Muller M, Heicappell R, Krause H, Straub B, Schrader M, Miller K: DNA-based detection of prostate cancer in urine after prostatic massage. Urology 2001, 58:335–338
25. Goessl C, Muller M, Heicappell R, Krause H, Miller K: DNA-based detection of prostate cancer in blood, urine, and ejaculates. Ann NY Acad Sci 2001, 945:51–58
26. Cairns P, Esteller M, Herman JG, Schoenberg M, Jeronimo C, Sanchez-Cespedes M, Chow NH, Grasso M, Wu L, Westra WB, Sidransky D: Molecular detection of prostate cancer in urine by GSTP1 hypermethylation. Clin Cancer Res 2001, 7:2727–2730
27. Lin X, Tascilar M, Lee WH, Vles WJ, Lee BH, Veeraswamy R, Asgari K, Freije D, van Rees B, Gage WR, Bova GS, Isaacs WB, Brooks JD, DeWeese TL, De Marzo AM, Nelson WG: GSTP1 CpG island hypermethylation is responsible for the absence of GSTP1 expression in human prostate cancer cells. Am J Pathol 2001, 159:1815–1826
28. Jeronimo C, Usadel H, Henrique R, Oliveira J, Lopes C, Nelson WG, Sidransky D: Quantitation of GSTP1 methylation in non-neoplastic prostatic tissue and organ-confined prostate adenocarcinoma. J Natl Cancer Inst 2001, 93:1747–1752
29. Maruyama R, Toyooka S, Toyooka KO, Virmani AK, Zochbauer-Muller S, Farinas AJ, Minna JD, McConnell J, Frenkel EP, Gazdar AF: Aberrant promoter methylation profile of prostate cancers and its relationship to clinicopathological features. Clin Cancer Res 2002, 8:514–519
30. Goessl C, Muller M, Heicappell R, Krause H, Schostak M, Straub B, Miller K: Methylation-specific PCR for detection of neoplastic DNA in biopsy washings. J Pathol 2002, 196:331–334
31. Chu DC, Chuang CK, Fu JB, Huang HS, Tseng CP, Sun CF: The use of real-time quantitative polymerase chain reaction to detect hypermethylation of the CpG islands in the promoter region flanking the GSTP1 gene to diagnose prostate carcinoma. J Urol 2002, 167:1854–1858
32. Jeronimo C, Varzim G, Henrique R, Oliveira J, Bento MJ, Silva C, Lopes C, Sidransky D: I105V polymorphism and promoter methylation of the GSTP1 gene in prostate adenocarcinoma. Cancer Epidemiol Biomarkers Prev 2002, 11:445–450
33. Brooks JD, Weinstein M, Lin X, Sun Y, Pin SS, Bova GS, Epstein JI, Isaacs WB, Nelson WG: CG island methylation changes near the GSTP1 gene in prostatic intraepithelial neoplasia. Cancer Epidemiol Biomarkers Prev 1998, 7:531–536
34. Esteller M, Corn PG, Urena JM, Gabrielson E, Baylin SB, Herman JG: Inactivation of glutathione S-transferase P1 gene by promoter hypermethylation in human neoplasia. Cancer Res 1998, 58:4515–4518
35. Vanheenders GJ, Gage WR, Hicks JL, B. vB, Aalders TW, Schalken JA, De Marzo AM: Intermediate cells in human prostate epithelium are enriched in proliferative inflammatory atrophy. Am J Pathol 2003, 162:29–37
36. Hayes JD, Pulford DJ: The glutathione S-transferase supergene family: regulation of GST and the contribution of the isoenzymes to cancer chemoprotection and drug resistance. Crit Rev Biochem Mol Biol 1995, 30:445–600
37. Kinzler KW, Vogelstein B: Cancer-susceptibility genes. Gatekeepers and caretakers. Nature 1997, 386:761–763
38. Henderson CJ, Smith AG, Ure J, Brown K, Bacon EJ, Wolf CR: Increased skin tumorigenesis in mice lacking pi class glutathione S-transferases. Proc Natl Acad Sci USA 1998, 95:5275–5280
39. Layton DW, Bogen KT, Knize MG, Hatch FT, Johnson VM, Felton JS: Cancer risk of heterocyclic amines in cooked foods: an analysis and implications for research. Carcinogenesis 1995, 16:39–52
40. Stuart GR, Holcroft J, de Boer JG, Glickman BW: Prostate mutations in rats induced by the suspected human carcinogen 2-amino-1-methyl-6-phenylimidazo[4,5-β]pyridine. Cancer Res 2000, 60:266–268
41. Shirai T, Sano M, Tamano S, Takahashi S, Hirose M, Futakuchi M, Hasegawa R, Imaida K, Matsumoto K, Wakabayashi K, Sugimura T, Ito N: The prostate: a target for carcinogenicity of 2-amino-1-methyl-6-phenylimidazo[4,5-β]pyridine (PhIP) derived from cooked foods. Cancer Res 1997, 57:195–198
42. Nelson CP, Kidd LC, Sauvageot J, Isaacs WB, De Marzo AM, Groopman JD, Nelson WG, Kensler TW: Protection against 2-hydroxyamino-1-methyl-6-phenylimidazo[4,5-β]pyridine cytotoxicity and DNA adduct formation in human prostate by glutathione S-transferase P1. Cancer Res 2001, 61:103–109
43. Nuovo GJ, Plaia TW, Belinsky SA, Baylin SB, Herman JG: In situ detection of the hypermethylation-induced inactivation of the p16 gene as an early event in oncogenesis. Proc Natl Acad Sci USA 1999, 96:12754–12759